Title

Cohesin Function in Cohesion, Condensation, and DNA Repair Is Regulated by Wpl1p via a Common Mechanism in Saccharomyces cerevisiae

Journal

Genetics, 208(1)

ISSN

0016-6731

Authors

Bloom, Michelle S
Koshland, Douglas
Guacci, Vincent

Publication Date

2018

DOI

10.1534/genetics.117.300537

Peer reviewed

Cohesin Function in Cohesion, Condensation, and DNA Repair Is Regulated by Wpl1p via a Common Mechanism in *Saccharomyces cerevisiae*

Michelle S. Bloom, Douglas Koshland,[1] and Vincent Guacci
Department of Molecular and Cell Biology, University of California, Berkeley, California 94720

ABSTRACT Cohesin tethers DNA to mediate sister chromatid cohesion, chromosome condensation, and DNA repair. How the cell regulates cohesin to perform these distinct functions remains to be elucidated. One cohesin regulator, Wpl1p, was characterized in *Saccharomyces cerevisiae* as a promoter of efficient cohesion and an inhibitor of condensation. Wpl1p is also required for resistance to DNA-damaging agents. Here, we provide evidence that Wpl1p promotes the timely repair of DNA damage induced during S-phase. Previous studies have indicated that Wpl1p destabilizes cohesin's binding to DNA by modulating the interface between the cohesin subunits Mcd1p and Smc3p. Our results suggest that Wpl1p likely modulates this interface to regulate all of cohesin's biological functions. Furthermore, we show that Wpl1p regulates cohesion and condensation through the formation of a functional complex with another cohesin-associated factor, Pds5p. In contrast, Wpl1p regulates DNA repair independently of its interaction with Pds5p. Together, these results suggest that Wpl1p regulates distinct biological functions of cohesin by Pds5p-dependent and -independent modulation of the Smc3p/Mcd1p interface.

KEYWORDS sister chromatid cohesion; condensation; DNA repair; cohesin; Wpl1

COHESIN, a member of the SMC family of protein complexes, is comprised of four subunits: Smc1p, Smc3p, Mcd1p (Scc1/Rad21), and Scc3p (SA/STAG). Cohesin mediates nuclear functions essential for both viability and the accurate transmission of genetic information, including sister chromatid cohesion, chromosome condensation, and repair of DNA damage (Onn *et al.* 2008). Cohesin is thought to perform these different functions through the spatial and temporal regulation of its ability to tether two genomic loci (Guacci *et al.* 1997; Michaelis *et al.* 1997; Hartman *et al.* 2000; Ström *et al.* 2007; Unal *et al.* 2007). Cohesin's DNA-binding and -tethering activities are regulated by factors including Eco1p (Ctf7p), Pds5p, and Wpl1p (Rad61p) (Skibbens *et al.* 1999; Tóth *et al.* 1999; Hartman *et al.* 2000; Rolef Ben-Shahar *et al.* 2008; Unal *et al.* 2008). How these regulatory factors interface with each other and with cohesin to promote its biological functions remains poorly understood.

Wpl1p was first implicated as a negative regulator of the cohesin complex, serving to inhibit both cohesion and condensation. Evidence that Wpl1p inhibits condensation stems from findings that the deletion of *WPL1* (*wpl1*Δ) restores both viability and condensation to cells lacking Eco1p function (*eco1*Δ) (Guacci and Koshland 2012), and that *wpl1*Δ cells prematurely condense their DNA (Lopez-Serra *et al.* 2013). Additionally, Wpl1p's role as an inhibitor of cohesion stems from findings that Wpl1p overexpression in human or yeast cells induces a partial cohesion loss (Gandhi *et al.* 2006; Lopez-Serra *et al.* 2013). Wpl1p is thought to inhibit cohesin function by removing it from DNA in a nonproteolytic manner (Gandhi *et al.* 2006; Kueng *et al.* 2006).

Recent biochemical studies suggest that Wpl1p destabilizes the interface between the N-terminus of Mcd1p and the base of the coiled-coil of Smc3p (Buheitel and Stemmann 2013; Beckouët *et al.* 2016). Additionally, mutating an Smc3p residue in the Smc3p/Mcd1p interface abolishes cohesin localization to centromere-proximal regions, providing *in vivo* support for a role for this interface (Gligoris *et al.* 2014). However, the biological function and regulation of

doi: https://doi.org/10.1534/genetics.117.300537
Manuscript received July 14, 2017; accepted for publication November 16, 2017; published Early Online November 20, 2017.
Available freely online through the author-supported open access option.
Supplemental material is available online at www.genetics.org/lookup/suppl/doi:10.1534/genetics.117.300537/-/DC1.
[1]Corresponding author: Department of Molecular and Cell Biology, University of California, Berkeley, 408 Barker Hall, Berkeley, CA 94720. E-mail: koshland@berkeley.edu

destabilization of the Smc3p/Mcd1p interface is poorly understood.

To limit Wpl1p inhibition, cohesin is acetylated by Eco1p at two conserved lysine residues on Smc3p (K112 and K113 in the budding yeast, *Saccharomyces cerevisiae*) (Rolef Ben-Shahar *et al.* 2008; Unal *et al.* 2008). Additionally, Pds5p helps to preserve Smc3p acetylation during and after S-phase, suggesting a common molecular mechanism for how Pds5p and Eco1p promote cohesion (Chan *et al.* 2013). These functions are also thought to promote condensation, as inactivation of either factor results in dramatic defects in both cohesion and condensation (Skibbens *et al.* 1999; Hartman *et al.* 2000). Furthermore, overexpression of Pds5p suppresses mutants containing *eco1-ts* alleles, and vice versa, supporting the idea that Pds5p and Eco1p promote cohesin function through a common molecular mechanism (Noble *et al.* 2006). Taken together, these data suggest that both Eco1p and Pds5p prevent Wpl1p-mediated antagonization of cohesion and condensation.

However, the function of Wpl1p and Pds5p in regulating cohesin is more complicated. In budding yeast, *wpl1*Δ cells display a partial cohesion defect, implicating Wpl1p as a positive factor required for the efficient establishment of cohesion (Rowland *et al.* 2009; Sutani *et al.* 2009; Guacci and Koshland 2012). However, the molecular differences between Wpl1p's positive and negative functions remain a mystery. Furthermore, Wpl1p and Pds5p form a complex that is capable of unloading of cohesin from DNA *in vitro* (Kueng *et al.* 2006; Murayama and Uhlmann 2015). This finding suggests that Pds5p inhibits cohesin in addition to its well-established role in promoting cohesin function. Consistent with this idea, in *Schizosaccharomyces pombe*, deletion of *PDS5* suppresses a deletion of the *ECO1* homolog, Eso1 (Tanaka *et al.* 2001). Moreover, in budding yeast, certain *pds5* alleles suppress the inviability of the *eco1-1* temperature-sensitive mutant, which has reduced cohesin acetylation (Rowland *et al.* 2009; Sutani *et al.* 2009). This suppression suggests that these *pds5* mutations inactivate an inhibitory activity of Pds5p. Together, these results suggest that Wpl1p and Pds5p can act both positively and negatively to regulate cohesin functions.

The complex regulation of Wpl1p on cohesin function raises important questions that we address in this study. First, are there additional roles of Wpl1p in regulating cohesin function? Does Wpl1p regulate all cohesin's biological functions through a common molecular mechanism? Finally, is Wpl1p's ability to form a complex with Pds5p important for any or all of Wpl1p's regulatory functions? The answers to these questions provide important new insights into cohesin regulation by Wpl1p and its interplay with Pds5p.

Materials and Methods

Yeast strains, media, and reagents

Yeast strains used in this study had an A364A background and their genotypes are listed in Supplemental Material, Table S1 in File S1. YPD liquid media was prepared containing 1% yeast extract, 2% peptone, and 2% dextrose, 0.01 mg/ml adenine. YPD solid media was prepared the same way as liquid media and contained 2% agar. Camptothecin (CPT) (Sigma [Sigma Chemical], St. Louis, MO) was made as a 10 mg/ml stock in dimethyl sulfoxide (DMSO) and added to a final concentration of 20 μg/ml in YPD solid or liquid media containing 25 mM pH 7.4 [4-(2-hydroxyethyl)-1-pipera-zineethanesulfonic acid (HEPES; Fisher Scientific, Fair Lawn, NJ)]. Next, 99% pure methyl methanesulfonate (MMS) (Sigma) was added to a final concentration of 0.01% in YPD solid media. MMS was diluted 1:10 in DMSO and added to YPD liquid media to a final concentration of 0.01%. Agar plates containing MMS were made within 2 days of use to prevent degradation. 5-FOA (US Biological Life Sciences, Salem, MA) was used at a final concentration of 1 g/liter in URA dropout plates supplemented with 50 mg/liter uracil (Sigma).

Dilution plating

Cells were grown to saturation in YPD liquid media at 30° (23° for temperature-sensitive strains) then plated in 10-fold serial dilutions. Cells were incubated on plates at relevant temperatures or containing drugs as described. For plasmid shuffle assays, cells were grown to saturation in YPD liquid media to allow loss of covering plasmid, then plated in 10-fold serial dilutions on YPD or 5-FOA media.

Cohesin and condensation time course

Cells were inoculated into 5 ml YPD starter cultures and incubated overnight at 23°, then starter cultures were used to inoculate into larger volumes of YPD and grown overnight to midlog phase (~0.2–0.3 OD). α-factor (Sigma) was added to midlog cultures (10^{-8} M final) and incubated for 3 hr to arrest cells in G1. Cells were released from G1 by washing 3× in YPD containing 0.2 μg/ml Pronase E, once in YPD, and then resuspended in YPD containing 15 μg/ml nocodazole (Sigma) and incubated at 23° for 3 hr to allow cell cycle progression until arrest in mid-M. To assess cohesion through separation of LacI-GFP foci, cells were fixed for 15–30 min in 4% paraformaldehyde (w/v) and 3.4% sucrose (w/v) solution, washed, and resuspended in 0.1 KPO_4 1.2 M sorbitol buffer, then stored at 4°.

For auxin treatment, time courses were performed as above, except that 3-indoleacetic acid (auxin; Sigma) was added to final concentration of 500 μM to α-factor-arrested cells from a 1 M stock solution in DMSO. Cells were then incubated for an additional 1 hr. Auxin (500 μM) was present in all YPD washes and the releasing media containing nocodazole.

CPT- and MMS-treatment time course

Cells were grown, arrested in G1, and released as described above. Upon release from α-factor, cells were split and resuspended into YPD containing either DMSO, 20 μg/ml CPT and 25 mM HEPES pH 7.4, or 0.01% MMS, and incubated at 23° to allow cell cycle progression. Ninety minutes after release,

α-factor was readded to cultures at 10^{-8} M to arrest in subsequent G1. Cells were harvested every 30 min and fixed in 70% ethanol. To assess chromosome segregation, fixed cells were washed and resuspended in 1× PBS containing DAPI.

For assessment of chromosome segregation when treated with MMS or CPT in nocodazole (G2/M) cells, cells were grown, arrested, and released from α-factor arrest into nocodazole in the absence of drugs, as described above. Cells were then released from nocodazole arrest by washing 3× in YPD. Cells were then split and resuspended into media containing α-factor at 10^{-8} M and either DMSO, 20 μg/ml CPT and 25 mM HEPES pH 7.4, or 0.01% MMS.

Fluorescence in situ hybridization (FISH)

Nocodazole-arrested cells were fixed and processed for FISH as previously described (Guacci and Koshland 1994; Guacci *et al.* 1997), except cells were stained with ProLong Gold Antifade Mountant with DAPI (Life Technologies, Carlsbad, CA) instead of propidium iodide.

Flow cytometry

To assess DNA content, cells were fixed in 70% ethanol. Fixed cells were washed twice in 50 mM sodium citrate (pH 7.2) and then treated with RNase A [50 mM sodium citrate (pH 7.2), 0.25 mg/ml RNase A, and 1% Tween-20 (v/v)] overnight at 37°. Proteinase K was then added to a final concentration of 0.2 mg/ml and samples were incubated at 50° for 2 hr. Samples were sonicated for 30 sec or until cells were adequately disaggregated. SYBR Green DNA I dye (Life Technologies) was then added at 1:20,000 dilution and samples were run on a Guava easyCyte flow cytometer (Millipore, Billerica, MA). For each time point, 20,000 events were captured. Quantification was performed using FlowJo analysis software.

Microscopy

Images were acquired with an Axioplan2 microscope [100× objective, numerical aperture (NA) 1.40; Zeiss [Carl Zeiss], Thornwood, NY] equipped with a Quantix charge-coupled device camera (Photometrics, Tucson, AZ).

Preparation of cells for immunoprecipitation

Cells were inoculated into 5 ml starter cultures and grown overnight at 23°. Strains were then inoculated into 60 ml cultures and grown to a final OD of 0.8. Twenty ODs were then harvested, washed in 1 × PBS, spun down, liquid aspirated, and cells were flash frozen in liquid N_2.

For CPT, untreated cells were grown to a final OD_{600} of 0.4. Next, 1 M HEPES pH 7.4 was added to cultures to a final concentration of 25 mM, 10 mg/ml CPT stock was added to cells to a final concentration of 20 μg/ml, and cells were incubated for 3 hr. Twenty ODs were then harvested and prepared as described above.

Immunoprecipitation

Cell lysates were prepared by bead beating for 30 sec with 1 min rest, 4× at 4° in GNK100 buffer (100 mM KCl, 20 mM HEPES pH 7.5, 0.2% NP40, 10% glycerol, and 2.5 mM $MgCl_2$) containing complete mini EDTA-free protease inhibitor (Roche), 5 mM sodium butyrate, 5 mM β-mercaptoethanol, 1 mM PMSF, and 20 mM b-glycerophosphate. Lysates were cleared of insoluble cell debris and then incubated with anti-FLAG antibody (Sigma) and Protein A dynabeads for 1 hr at 4°. Dynabeads were then washed 4× with GNK100 buffer with additives, as described above, containing 100 μM MG132. Samples were then run on SDS-PAGE gels and analyzed through western blot analysis.

Preparation of bulk chromatin pellets

Cells were inoculated into 5 ml YPD starter culture and incubated overnight at 23°. Cells were inoculated from starter cultures into fresh YPD to grow overnight at 23° to midlog phase, then 15 μg/ml nocodazole was added and cells were incubated for 3 hr to arrest cultures in mid-M-phase. Cells were processed for bulk chromatin pelleting as described in Ciosk *et al.* (2000), with the modification that spheroplasted cells were washed three times in 0.4 M sorbitol, 50 mM HEPES/KOH pH 7.5, 100 mM KCl, and 2.5 mM $MgCl_2$ before lysis.

Data availability

Strains are available on request.

Results

Wpl1p is necessary to mitigate CPT- and MMS-induced cell cycle delay

Wpl1p has been implicated in regulating cohesin function in both cohesion and condensation. However, Wpl1p function in another cohesin-regulated process, DNA repair, has not been well characterized. The *wpl1/rad61* mutant was originally identified in a budding yeast screen due to its weak sensitivity to ionizing radiation (Game *et al.* 2003). Subsequent work showed that *wpl1*Δ cells have reduced viability when grown on plates containing either the topoisomerase I inhibitor CPT (10–15 μg/ml) or the alkylating agent MMS (Sutani *et al.* 2009; Guacci and Koshland 2012; Guacci *et al.* 2015). In contrast, *eco1*Δ *wpl1*Δ cells exhibited severe sensitivity to both CPT and MMS (Sutani *et al.* 2009; Guacci and Koshland 2012). *wpl1*Δ cells have a modest cohesion defect, whereas *eco1*Δ *wpl1*Δ cells have a dramatic cohesion defect (Sutani *et al.* 2009; Guacci and Koshland 2012). The hypersensitivity of *eco1*Δ *wpl1*Δ cells to CPT and MMS is likely due to the severe cohesion defect impairing use of the sister chromatid as a template for DNA repair. These results clearly indicate that Wpl1p promotes resistance to DNA-damaging agents, but how it does so is unknown. To gain insight into this Wpl1p function, we analyzed how loss of Wpl1p affected viability and chromosome segregation under DNA-damaging conditions.

We first revisited the sensitivity of *wpl1*Δ cells by analyzing their growth on media containing higher concentrations of

CPT than had been previously tested. We compared the growth of wild-type, *wpl1*Δ, and *eco1*Δ *wpl1*Δ cells on media containing 20 μg/ml CPT. As expected, *eco1*Δ *wpl1*Δ cells were unable to grow even after 5 days, confirming that Eco1p plays a critical role in surviving DNA damage (Figure 1A). Interestingly, after 3 days of growth on CPT, *wpl1*Δ cells appeared to have much lower viability than wild-type cells. However, by 5 days, *wpl1*Δ cells exhibited similar viability to wild-type cells, but formed smaller colonies, indicating slower growth (Figure 1A). Given this delayed growth phenotype, we then examined *wpl1*Δ cell growth on MMS-containing plates. Consistent with our findings for CPT, *wpl1*Δ cell growth on MMS was significantly delayed compared to wild-type cells, taking several days to form colonies, but the overall viability was similar to wild-type cells (Figure 1B). The similar viability but slower growth seen in *wpl1*Δ cells subjected to DNA damage suggests that Wpl1p may promote efficient DNA repair.

We further characterized the kinetics of DNA-damage repair, by analyzing how CPT and MMS treatment affected cell cycle progression of wild-type and *wpl1*Δ cells. We utilized the extent and duration of a drug-induced cell cycle delay as an indirect measure of DNA damage and repair. We synchronized wild-type and *wpl1*Δ cells in G1 with α-factor, and then released cells into media either containing no drugs (DMSO), CPT (20 μg/ml), or MMS (0.01%) (*Materials and Methods*). Once cells budded, we reintroduced α-factor into the media to enable cells to progress through the cell cycle and then rearrest in the following G1. Aliquots of cells were collected every 30 min after G1 release and analyzed for bud morphology, DNA content, and chromosome segregation (Figure 2A).

We first compared cell cycle progression of wild-type and *wpl1*Δ cells when treated with DMSO (control) and either CPT or MMS by analyzing DNA content using flow cytometry. Progression through S-phase (transitioning from 1C to 2C) was the same for drug-treated cells and DMSO control cells (Figure S1, A and B in File S1). However, in CPT-treated *wpl1*Δ cells, the 2C DNA peak persisted longer than in either CPT-treated wild-type cells or DMSO-treated cells of either genotype (Figure S1A in File S1; 180–240 min). MMS-treated wild-type and *wpl1*Δ cells both exhibited 2C DNA peaks that persisted longer than DMSO controls, but the delay was more pronounced in *wpl1*Δ cells (Figure S1B in File S1; 150–240 min). These results suggest that *wpl1*Δ cells delay in mitosis because of persisting DNA damage generated by either CPT or MMS, which activates the G2/M DNA-damage checkpoint.

We further characterized the CPT- and MMS-generated G2/M delays by examining bud and DNA morphologies of these cells. During an unperturbed cell cycle in yeast, DNA replication is completed when the bud is small and a single nuclear DNA mass bearing all the chromosomes is present. As the cell cycle progresses, the bud grows to medium size while mitosis quickly ensues. As chromosomes segregate, two separated DNA masses of equal size can be distinguished, one in the mother cell and one in the bud (telophase cells). If cells

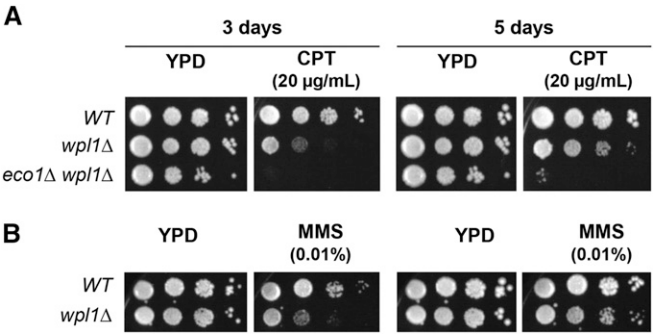

Figure 1 Wpl1p promotes proper growth on CPT and MMS media. (A) *wpl1*Δ cells grow slowly on media containing camptothecin (CPT). Haploid wild-type (*WT*) (VG3349-1B), *wpl1*Δ (VG3360-3D), and *eco1*Δ *wpl1*Δ (VG3503 #4) cells were grown to saturation in YPD at 23°, then plated in 10-fold serial dilutions on YPD alone or containing 20 μg/ml CPT. Plates were incubated at 23° and assessed at 3 and 5 days postplating. (B) *wpl1*Δ cells grow slowly on media containing MMS. Haploid *WT* (VG3349-1B) and *wpl1*Δ (VG3360-3D) cells were grown to saturation in YPD at 23°, then plated in 10-fold serial dilution on YPD alone or containing 0.01% MMS. Plates were incubated at 23° and assessed at 3 and 5 days post plating.

stall prior to anaphase, the undivided nucleus remains at the bud neck while the bud continues to grow, giving rise to large-budded cells with unsegregated chromosomes, seen as a single DNA mass (G2/M cells) (Figure 2A; Hartwell 1974). As expected, control DMSO-treated wild-type and *wpl1*Δ cells had few large-budded G2/M cells, as most cells entered telophase when buds were midsized, consistent with no cell cycle delay (Figure 2, B and C, left panels). By 150 min post-release, most cells were in telophase (large-budded with divided nuclei). The number of telophase cells declined as cells underwent cytokinesis, and most cells were arrested in G1 by 210 min (Figure 2, B and C, left panels).

When treated with CPT, both wild-type and *wpl1*Δ cultures exhibited a large increase in the amount of large-budded G2/M cells (~40% of cells), and few telophase cells were seen at 120 min postrelease compared to their DMSO-treated counterparts (Figure 2B, right panels). The similar G2/M cell cycle delays of both wild-type and *wpl1*Δ cells were consistent with both initially experiencing the same level of DNA damage when treated with CPT. Wild-type cells quickly overcame this delay, as seen by the high level of telophase cells at 150 and 180 min. Additionally, most wild-type cells had exited mitosis by 240 min (Figure 2B, top-right panel). In contrast, the amount of *wpl1*Δ cells stalled in G2/M increased until 150 min, with a significant amount remaining stalled through 240 min (Figure 2B, bottom-right panel). Eventually, most *wpl1*Δ cells entered telophase and exited mitosis, indicating that the CPT-induced damage was repaired.

Similar to CPT-treated cells, wild-type and *wpl1*Δ cells treated with MMS exhibited a G2/M delay to similar degrees, as ~50% of cells were large-budded with undivided nuclei 120 min after release (Figure 2C, right panels). However, ~50% of wild-type cells entered telophase by 150–180 min and few G2/M cells remained. In contrast, *wpl1*Δ cells were

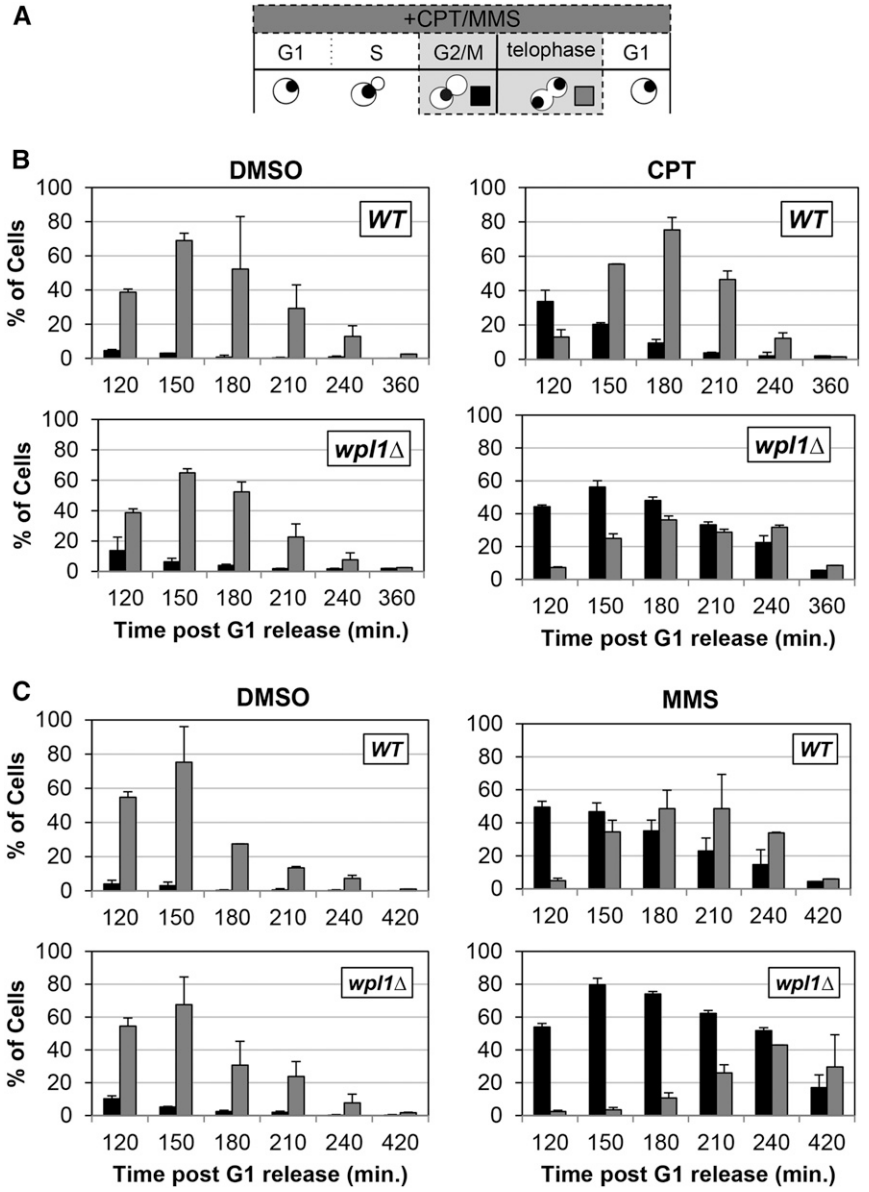

Figure 2 Wpl1p promotes recovery from G2/M delays generated by exposure to the DNA-damage-inducing agents camptothecin (CPT) and MMS. (A) Schematic of time course and analysis of cell cycle progression for untreated and CPT- or MMS-treated cells in (B and C). Wild-type (*WT*) (VG3349-1B) and *wpl1*Δ (VG3360-3D) cells were grown to midlog phase in YPD at 23°, arrested in G1 by addition of α-factor, then released from G1 into YPD (*Materials and Methods*). At the time of release from G1, cells were split into two aliquots: either CPT (final 20 μg/ml) or MMS (final 0.01%) was added to one and DMSO was added to the other. Once most cells had entered S-phase (90 min after release from G1), α-factor was added to ensure cells would progress through one cell cycle and rearrest in G1. Aliquots were taken every 30 min and fixed in 70% ethanol. Fixed cells were stained with DAPI to detect chromosomal DNA for scoring. Cells were scored for bud morphology (unbudded, small–medium bud, or large bud) and whether they contained a single DAPI chromosomal mass or two DAPI masses. (B) *wpl1*Δ cells grown in the presence of CPT from G1 onward exhibit a prolonged mitotic delay. *WT* (VG3349-1B) and *wpl1*Δ (VG3360-3D) cells were synchronously released from G1, as described (A), in YPD media buffered with 25 mM HEPES pH 7.4 containing DMSO alone or with 20 μg/ml CPT (*Materials and Methods*). Graphs show the percentage of large-budded cells with a single DNA mass (G2/M; black) or two DNA masses (telophase; gray). (C) *wpl1*Δ cells grown in the presence of MMS from G1 onward exhibit a prolonged mitotic delay. *WT* (VG3349-1B) and *wpl1*Δ (VG3360-3D) cells were synchronously released from G1, as described in (B), except that YPD media (unbuffered) contained DMSO alone or 0.01% MMS. Cells were collected, processed, and scored as described in (A). Graphs show the percentage of large-budded cells with a single DNA mass (G2/M; black) or two DNA masses (telophase; gray).

slow to enter telophase, and the fraction of G2/M cells increased by 150 min and remained elevated through 240 min (Figure 2C, right panels). Eventually, almost all *wpl1*Δ cells completed mitosis. Together, these results show that both CPT and MMS treatment cause an initial delay in segregation in both wild-type and *wpl1*Δ cells, from which they eventually recover. However, *wpl1*Δ cells experience a prolonged delay, which most likely results from defects in the timely repair of DNA damage.

CPT-mediated damage is thought to cause double-strand breaks (DSBs) when toposiomerase I-induced single-strand nicks encounter replication machinery during S-phase (Avemann *et al.* 1988; Strumberg *et al.* 2000; Saleh-Gohari *et al.* 2005). Additionally, MMS is thought to cause DNA damage through stalling replication forks during S-phase. Thus, our results implicate Wpl1p as being important in G2/M-phase for the repair of damage generated during S-phase. To test whether the exacerbated delay observed in *wpl1*Δ cells was due to the DNA damage generated during S-phase, we allowed cultures of wild-type and *wpl1*Δ cells to progress synchronously through S-phase in the absence of either CPT or MMS, and arrest in G2/M by the addition of the microtubule poison nocodazole. Upon release from nocodazole, cultures were split, and either CPT or MMS was added to one aliquot while DMSO was added to the other. We then monitored progression every 30 min through mitosis and cytokinesis in either the presence or absence of CPT or MMS. α-factor was added to the cultures to prevent progression of cells beyond the ensuing G1 (Figures S2A and S3A in File S1). Upon release from nocodazole, wild-type and *wpl1*Δ cells segregated their chromosomes with similar kinetics when treated with either DMSO or CPT (Figure S2, B and C in File S1). Similarly, MMS addition to nocodazole-arrested cultures failed to induce a cell cycle delay (Figure S3, B and C

in File S1). Thus, the drug-induced delay in the initiation of chromosome segregation in *wpl1*Δ cells required the presence of either CPT or MMS prior to M-phase. Taken together, these results suggest that Wpl1p is important for the efficient repair of multiple types of DNA damage induced during S-phase.

The Pds5p N-terminus and the Smc3p/Mcd1p interface regulate the inhibition of condensation

Our findings, along with those of previous studies, suggest that Wpl1p's regulation of diverse cohesin functions is complicated, that Wpl1p forms a complex with Pds5p, and that Wpl1p can destabilize the interface between the N-terminus of Mcd1p and the base of the coiled-coil of Smc3p (Shintomi and Hirano 2009; Chan *et al.* 2012; Beckouët *et al.* 2016). These results provided insights into the molecular mechanisms of Wpl1p function that led us to use two approaches to parse how Wpl1p distinguishes its functions in the regulation of cohesin. The first approach was to understand the relationship between Pds5p and Wpl1p. The second utilized an *SMC3-MCD1* fusion to assess the consequences of blocking the destabilization of the Smc3p/Mcd1p interface.

The ability of *wpl1*Δ to restore viability to cells lacking Eco1p function (*eco1*Δ) was previously shown (Rowland *et al.* 2009; Sutani *et al.* 2009; Feytout *et al.* 2011). Our further analysis showed that *wpl1*Δ suppressed the condensation defect of an *eco1*Δ mutant, but not the cohesion defect (Guacci and Koshland 2012). This result is consistent with the idea that abrogating Wpl1p-mediated inhibition of condensation is essential in Eco1p-deficient cells. Given that Wpl1p and Pds5p form a complex, we wondered whether they cooperate to inhibit condensation. Functional cooperation between Pds5p and Wpl1p is suggested by the fact that *wpl1*Δ and specific N-terminal *pds5* mutant alleles restore viability to *eco1-ts* cells that have reduced acetylase activity (Rowland *et al.* 2009; Chan *et al.* 2012). We further explored this relationship by assessing whether three of these N-terminal *pds5* alleles (*pds5-S81R*, *pds5-P89L*, and *pds5-E181K*) shared all the phenotypes characteristic of a *wpl1*Δ.

We first tested whether these *pds5* alleles could suppress *eco1*Δ inviability as a *wpl1*Δ does. For this purpose, we constructed strains where *pds5-S81R*, *pds5-P89L*, or *pds5-E181K* was the sole *pds5* allele in cells. We then generated *ECO1* shuffle strains in these *pds5* mutants and in a wild-type strain by introducing a centromere plasmid containing *ECO1* and *URA3* (*ECO1 CEN URA3*), then deleting *ECO1* from its endogenous locus (*eco1*Δ). Counterselection against cells containing the *ECO1 URA3 CEN* plasmid by plating on media containing 5-FOA revealed whether any of the *pds5 eco1*Δ double-mutants were viable.

As expected, cells containing wild-type *PDS5* and *eco1*Δ could not grow on 5-FOA, as *ECO1* is an essential gene. In contrast, both the *pds5-S81R* and *pds5-P89L* alleles enabled robust growth on 5-FOA, indicating suppression of *eco1*Δ (Figure 3A). Consistent with our findings, previous results also showed that *pds5-P89L* restored viability to *eco1*Δ (Sutani *et al.* 2009). In contrast, *pds5-E181K* did not support viability to *eco1*Δ (Figure 3A). To determine whether the inability of *pds5-E181K* to restore viability to *eco1*Δ was due to weak suppressor activity, we rebuilt *pds5-E181K* into a strain containing the *eco1-203* temperature-sensitive allele. At the restrictive temperature, 34°, *pds5-E181K eco1-203* cells grew (Figure S4A in File S1), consistent with a previous report in which *pds5-E181K* suppressed the inviability of the *eco1-1* temperature-sensitive allele (Rowland *et al.* 2009). Thus, *pds5-S81R* and *pds5-P89L* are akin to a *wpl1*Δ as they suppress an *eco1*Δ, whereas *pds5-E181K* can only suppress inviability when Eco1p function is reduced but not abolished.

A second phenotype characteristic of *wpl1*Δ cells is restoration of condensation but not cohesion to *eco1*Δ cells (Guacci and Koshland 2012). This pattern of suppression distinguishes the inactivation of Wpl1p function from *smc1* and *smc3* suppressor mutants, which partially restore cohesion in *eco1* mutants (Çamdere *et al.* 2015; Guacci *et al.* 2015). To test whether these *pds5* N-terminal alleles mimicked the *wpl1*Δ phenotype, we assessed chromosome condensation in *pds5-S81R eco1*Δ and *pds5-P89L eco1*Δ cells arrested in mid-M-phase. We utilized a standard method for assessing yeast chromosome condensation by monitoring the repetitive *rDNA* locus (Guacci and Koshland 1994; Guacci *et al.* 1997). The *rDNA* locus is located in the nucleolus and protrudes from the bulk chromosomal mass, making it easy to monitor its condensation state. A condensed *rDNA* locus forms a distinct loop structure, while decondensed *rDNA* locus form a "puff" morphology (Figure 3B; *Materials and Methods*) (Guacci *et al.* 1993; Guacci and Koshland 1994). We analyzed the morphology of the *rDNA* in cells synchronously arrested in mid-M-phase using nocodazole (Figure 3B). Since *eco1*Δ cells are not viable, we used an *ECO1-AID* strain as a control for decondensation in cells depleted for Eco1p activity. The *ECO1-AID* strain was treated the same as other strains, except that 500 μM auxin was added to the media to induce *ECO1-AID* depletion from G1 through mid-M-phase arrest. Most wild-type (*PDS5*) cells that arrested in mid-M had condensed *rDNA* loops, so few had decondensed *rDNA*, whereas > 80% of *ECO1-AID* cells had decondensed *rDNA* (Figure 3C). Most *pds5-S81R eco1*Δ and *pds5-P89L eco1*Δ cells had condensed *rDNA* loops, so only ∼20–30% of cells exhibited decondensed *rDNA* loci (Figure 3C). This result is similar to what was previously reported for *eco1*Δ *wpl1*Δ cells (Guacci and Koshland 2012). Thus, *pds5-S81R* and *pds5-P89L*, like *wpl1*Δ, suppress the condensation defect engendered by loss of Eco1p activity.

We next assessed sister chromatid cohesion in *pds5-S81R eco1*Δ and *pds5-P89L eco1*Δ double-mutant cells synchronously arrested in mid-M. We monitored cohesion at either a chromosome IV *CEN*-distal or *CEN*-proximal locus by integration of LacO repeats at either the *LYS4* or the *TRP1* locus, respectively, in cells containing LacI-GFP (*Materials and Methods*). Cells containing a single LacI-GFP focus indicated cohesion, whereas cells containing two LacI-GFP foci indicated a loss of cohesion (Figure 3B). As expected from our

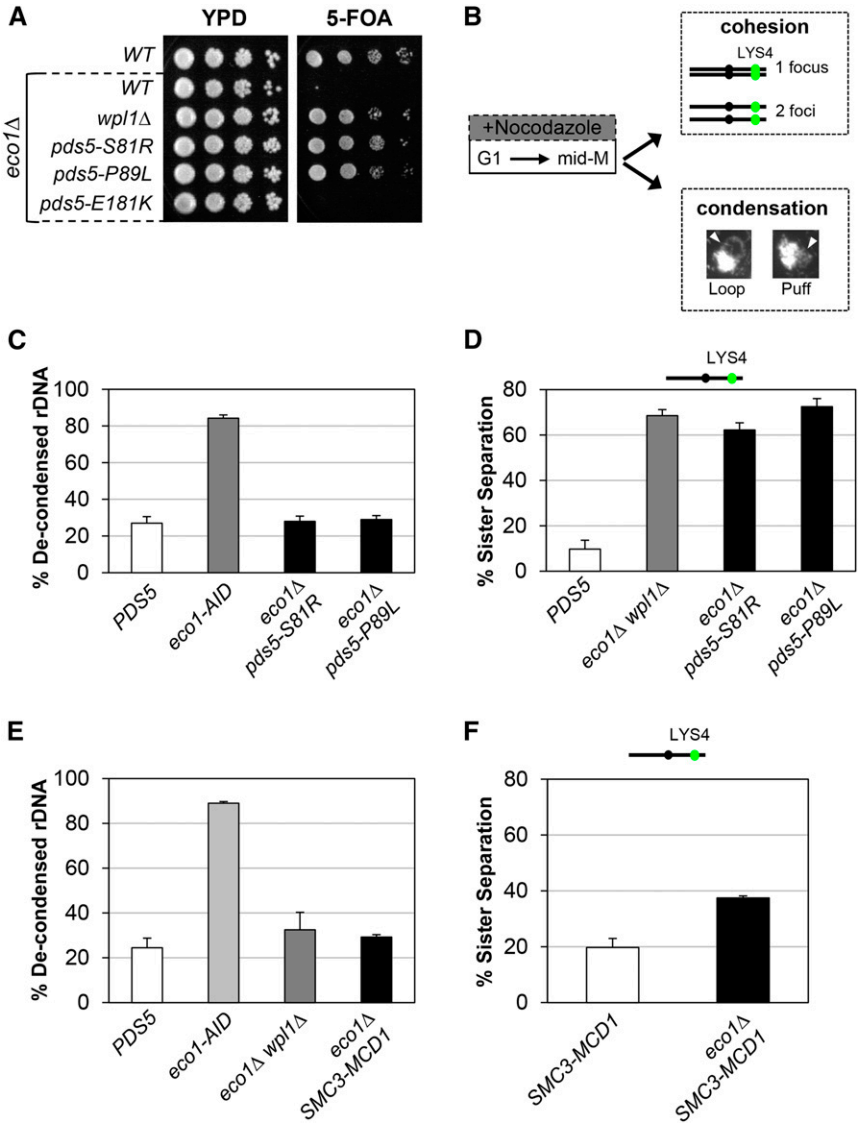

Figure 3 *pds5* N-terminal mutants and *SMC3-MCD1* fusion suppress inviability of *eco1*Δ through restoration of condensation. (A) Plasmid shuffle assay to assess viability of *pds5* N-terminal mutants in the *eco1*Δ background. Plasmid pBS1030 (*ECO1 CEN URA3*) is present in haploid wild-type (*WT*) (VG3349-1B), *eco1*Δ (VG3499-1B), *eco1*Δ *wpl1*Δ (VG3503 #4), *eco1*Δ *pds5-S81R* (MSB138-1K), *eco1*Δ *pds5-P89L* (MSB139-2J), and *eco1*Δ *pds5-E181K* (MSB147-1A) strains. Cells were grown to saturation in YPD media at 23°, plated at 10-fold serial dilutions on YPD or 5-FOA media, and then incubated for 3 days at 23°. 5-FOA selects for loss of pBS1030 (*ECO1 CEN URA3*). (B) Schematic of time course and analysis of cohesion and condensation. Cells were synchronously arrested in mid-M-phase as described in the *Materials and Methods*. Cells were processed for cohesion analysis of LacI-GFP at the *CEN*-distal *LYS4* locus and *CEN*-proximal *TRP1*, and for condensation by FISH methodology (*Materials and Methods*). (C) *pds5-S81R* and *pds5-P89L* restore condensation in *eco1*Δ cells. *PDS5* (VG3349-1B), *eco1-AID* (*VG3633-2D*), *eco1*Δ *pds5-S81R* (MSB138-1K), and *eco1*Δ *pds5-P89L* (MSB139-2J) were arrested in G1 using α-factor, then synchronously arrested in mid-M-phase using nocodazole as described in the *Materials and Methods*. From G1 through mid-M-phase, 500 μM auxin was present in the media of the *eco1-AID* strain. Cells were fixed and processed for FISH (*Materials and Methods*). Chromosome condensation was assessed by morphology of the *rDNA* locus and cells were scored for condensed *rDNA* (loops) and defective condensation (puffs). The percentage of cells with defective *rDNA* condensation (decondensed) is plotted. (D) *pds5-S81R eco1*Δ and *pds5-P89L eco1*Δ double-mutants have a dramatic defect on cohesion. *PDS5* (VG3349-1B), *eco1*Δ *wpl1*Δ (VG3503 #4), *eco1*Δ *pds5-S81R* (MSB138-1K), and *eco1*Δ *pds5-P89L* (MSB139-2J) cells were synchronously arrested in mid-M-phase using nocodazole (*Materials and Methods*). Cells were scored for cohesion (one GFP focus) and loss of cohesion (two GFP foci; sister separation) at the CEN-distal *LYS4* locus. The percentage of cells lacking cohesion (sister separation) is shown. (E) *SMC3-MCD1* fusion promotes condensation in *eco1*Δ cells. *WT* (VG3349-1B), *eco1-AID* (*VG3633-2D*), *eco1*Δ *wpl1*Δ (VG3502 #A), and *eco1*Δ *SMC3-MCD1* (MSB249-3A) were synchronously arrested in mid-M-phase (*Materials and Methods*). From G1 through mid-M-phase, 500 μM auxin was present in the media of the *eco1-AID* strain. Cells were fixed and processed for FISH to assess *rDNA* condensation (loops) and defective condensation (puffs), as described in (C). The percentage of cells with defective *rDNA* condensation (decondensed) is plotted. (F) *SMC3-MCD1* fusion partially restores cohesion to *eco1*Δ cells. *SMC3-MCD1* (VG3940-2D) and *eco1*Δ *SMC3-MCD1* (MSB249-3A) were synchronously arrested in mid-M-phase using nocodazole (*Materials and Methods*). Cells were scored for cohesion (one GFP focus) and loss of cohesion (two GFP foci; sister separation) at the CEN-distal *LYS4* locus as described in (B). The percentage of cells lacking cohesion (sister separation) is shown. The strains in this panel and in Figure 4C were analyzed for cohesion loss in the same experiment. The data were separated for clarity of presentation, and the *SMC3-MCD1* cohesin data are presented here and in Figure 4C.

previous studies (Guacci and Koshland 2012), most sister chromatids remained tethered in wild-type cells, whereas ~70% of *eco1*Δ *wpl1*Δ cells exhibited separated sister chromatids at both loci (Figure 3D and Figure S4B in File S1). The *pds5-S81R eco1*Δ and *pds5-P89L eco1*Δ cells exhibited high levels of separated sisters at both *CEN*-proximal and distal loci, similar to that seen in *eco1*Δ *wpl1*Δ cells (Figure 3D and Figure S4B in File S1). Additionally, the *pds5-E181K eco1-203* double-mutant and *eco1-203* single-mutant strains also had high levels of sister separation when monitored at the restrictive temperature, 34° (Figure S4C in File S1). Thus, the *pds5* N-terminal suppressor mutants behave like *wpl1*Δ, as they restore viability and condensation but not cohesion to *eco1*Δ or *eco1-ts* cells.

The defects in cohesin function observed in *wpl1*Δ cells, along with evidence that Wpl1p destabilizes the interface between Smc3p and Mcd1p, suggest that this activity is important for promoting one or more of cohesin's biological functions. If so, one or more of these functions would be compromised when Wpl1p's destabilization activity was blocked by covalently fusing Smc3p to Mcd1p. Previously, a construct in which Smc3p was fused to the N-terminus of

Mcd1p (*SMC3-MCD1*) was shown to support viability when providing the sole sources of both Smc3p and Mcd1p in the cell (Gruber *et al.* 2006). Additionally, this fusion protein was able to restore viability to an *eco1*Δ mutant (Chan *et al.* 2012). This suppression of *eco1*Δ inviability suggested that the *SMC3-MCD1* fusion may suppress Wpl1p's ability to inhibit condensation.

To assess this possibility directly, we examined whether an *SMC3-MCD1* fusion would suppress the condensation defect of an *eco1*Δ like a *wpl1*Δ does. We generated a strain in which the *SMC3-MCD1* fusion was the sole source of both *SMC3* and *MCD1*. Consistent with previous reports, we were then able to delete *ECO1* (*eco1*Δ) in this background. We examined *rDNA* condensation in wild-type, *SMC3-MCD1*, and *SMC3-MCD1 eco1Δ* cells that were synchronously arrested in M-phase (*Materials and Methods*). As before, we used an *ECO1-AID* strain as a control for decondensation. As expected, most wild-type cells had condensed *rDNA* loops, with few displaying decondensed *rDNA*, whereas most *eco1-AID* cells had decondensed *rDNA* (Figure 3E). Only a small percentage (∼25%) of *SMC3-MCD1 eco1*Δ cells had decondensed *rDNA*, similar to what was observed in wild-type and *eco1*Δ *wpl1*Δ cells, indicating that the *SMC3-MCD1* fusion, like *wpl1*Δ, is able to restore condensation to cells lacking Eco1p (Figure 3E).

We next assessed whether the *SMC3-MCD1* fusion restores cohesion to *eco1*Δ by comparing the *SMC3-MCD1* and *SMC3-MCD1 eco1*Δ strains. Strains were synchronously arrested in mid-M-phase (*Materials and Methods*) and cohesion was assessed at the *CEN*-distal *LYS4* locus. *SMC3-MCD1* exhibited a mild cohesion defect of ∼20%. However, *SMC3-MCD1 eco1*Δ cells had an increased cohesion defect of ∼40% (Figure 3F). This cohesion defect at the *CEN*-distal *LYS4* locus was less severe than the 70% seen in *eco1*Δ *wpl1*Δ cells and the 70–80% seen in *eco1-AID* cells (Figure 3D; Guacci and Koshland 2012; Çamdere *et al.* 2015; Guacci *et al.* 2015). Therefore, the Smc3p-Mcd1p fusion protein can partially restore cohesion to *eco1*Δ cells, unlike *wpl1*Δ or the pds5 N-terminal mutants, which are unable to restore any cohesion.

The Pds5p N-terminus and the Smc3p/Mcd1p interface promote cohesion establishment

A third phenotype characteristic of *wpl1*Δ cells is their partial defect in cohesion establishment (Guacci and Koshland 2012). Budding yeast Pds5p-defective cells were already known to have a severe cohesion maintenance defect (Hartman *et al.* 2000; Panizza *et al.* 2000; Stead *et al.* 2003; Eng *et al.* 2014). The difference in the timing and severity of the cohesion defects suggested that Wpl1p and Pds5p might promote cohesion by distinct mechanisms. Alternatively, Pds5p might promote cohesion by two mechanisms, one dependent on Wpl1p and the other independent of Wpl1p. The phenotypic similarity between *wpl1*Δ and the N-terminal alleles of *pds5* described above suggested that the N-terminus of Pds5p might be involved in a Wpl1p-dependent pathway. We tested this possibility by monitoring the ability of *pds5-S81R*, *pds5-P89L*, and *pds5-E181K* to mediate cohesion, either in the presence or in the absence of *WPL1*.

We first assessed cohesion in the *pds5* N-terminal mutants in an otherwise wild-type background (*WPL1*) in cells synchronously arrested in mid-M-phase. When cohesion was monitored at both *CEN*-proximal and *CEN*-distal loci, all three *pds5* N-terminal mutants exhibited cohesion defects of ∼20 and ∼30%, respectively, similar to that of *wpl1*Δ (Figure 4A and Figure S5A in File S1). The *pds5-P89L* mutant was previously shown to have a similar small cohesion defect at the *URA3* locus (Sutani *et al.* 2009). Additionally, the *pds5* N-terminal mutants lost cohesion with similar kinetics as *wpl1*Δ cells progressed from S- to M-phase (Figure S5B in File S1). These similarities suggest that Wpl1p and the Pds5p N-terminal domain act in a common pathway to promote efficient cohesion establishment.

To more directly assess whether Wpl1p and the Pds5p N-terminus function in a common pathway to promote cohesion, we examined cohesion in *wpl1*Δ *pds5* N-terminal double-mutants. If Wpl1p and the Pds5p N-terminus function in a common pathway, we would expect the double-mutant to have cohesion defects similar to each single-mutant alone. In contrast, if Wpl1p and the Pds5p N-terminus function in distinct pathways, we would expect the double-mutants to have additive increases in cohesion defects approaching 60–70%. The cohesion defects of all three *pds5 wpl1*Δ double-mutants (*pds5-S81R wpl1*Δ, *pds5-P89L wpl1*Δ, and *pds5-E181K wpl1*Δ) were ∼30–40% when measured at *LYS4*, and ∼20–30% when measured at *TRP1*. These cohesion defects were the same or only slightly higher than *pds5* single-mutants (*pds5-S81R*, *pds5-P89L*, and *pds5-E181K*) alone or *wpl1*Δ alone (Figure 4A and Figure S5A in File S1). The similar partial cohesion defects between *pds5* single-mutants and *pds5 wpl1*Δ double-mutants suggest that the Pds5p N-terminus and Wpl1p promote cohesion through a common pathway. These results suggest that Wpl1p interacts functionally with Pds5p, both to inhibit condensation and to efficiently promote cohesion.

The cohesion defect that we observed in *SMC3-MCD1* fusion was similar to that of *wpl1*Δ cells (compare Figure 3F and Figure 4A). Similar results for both the *SMC3-MCD1* fusion and the *wpl1*Δ strains were previously reported at the more *CEN*-proximal *URA3* locus (Gruber *et al.* 2006; Rowland *et al.* 2009). Given that Wpl1p is thought to destabilize the Smc3p/Mcd1p interface, these similarities suggested that the cohesion defect could be due to an inability of Wpl1p to modulate the interface in the fusion. Therefore, we reexamined cohesion in the *wpl1*Δ mutant and the *SMC3-MCD1* fusion in the same experiment. *SMC3-MCD1* and *wpl1*Δ did indeed have similar moderate defects in cohesion of ∼20–30% at the *CEN*-distal *LYS4* locus when cells were arrested in mid-M-phase (Figure 4B). If the moderate cohesion defect in *SMC3-MCD1* cells was due to an inability of Wpl1p to modulate this interface, then deleting *WPL1* in the *SMC3-MCD1* strain should have no further impact on the cohesion defect. Indeed, the *SMC3-MCD1 wpl1*Δ strain had a similar partial

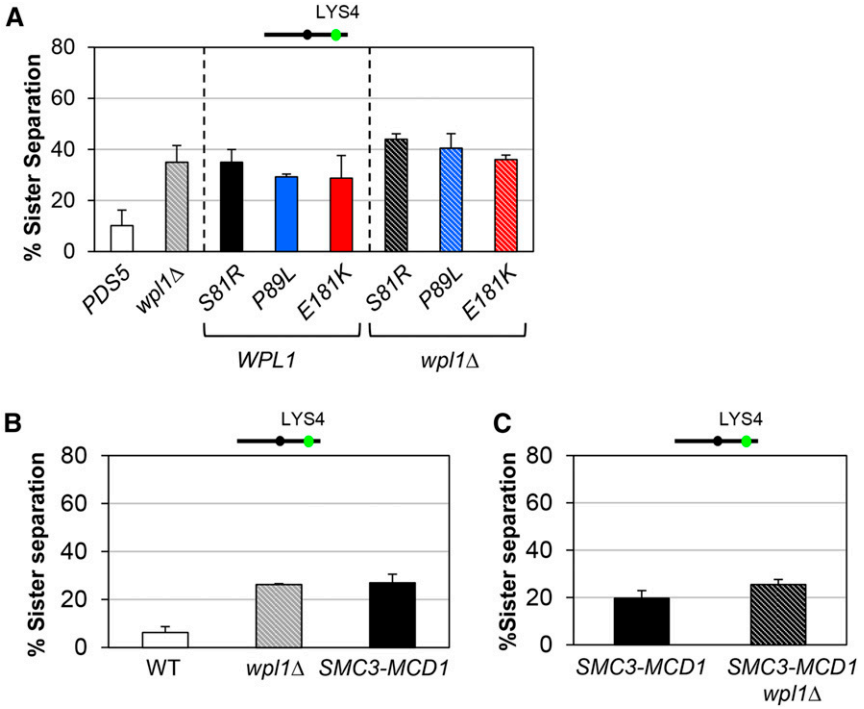

Figure 4 *pds5* N-terminal mutants and *SMC3-MCD1* fusion are defective for Wpl1p-mediated cohesion. (A) *pds5* N-terminal mutants have a modest cohesion defect similar to *wpl1*Δ alone or to *pds5 wpl1*Δ double-mutants. Strains *PDS5* (VG3349-1B), *wpl1*Δ (VG3360-3D), *pds5-S81R* (MSB183-1A), *pds5-P89L* (MSB184-3A), *pds5-E181K* (MSB101-3C), *pds5-S81R wpl1*Δ (MSB133-3C), *pds5-P89L wpl1*Δ (MSB134-1L), and *pds5-E181K wpl1*Δ (MSB223-1A) were synchronously arrested in mid-M-phase and scored for cohesion at the *CEN*-distal *LYS4* locus, as described in Figure 3D. The percentage of cells lacking cohesion (sister separation) is shown. (B) *SMC3-MCD1* has a similar modest cohesion defect to *wpl1*Δ. *PDS5* (VG3349-1B), *wpl1*Δ (VG3360-3D), and *SMC3-MCD1* (VG3940-2D) were synchronously arrested in mid-M-phase and scored for cohesion at *CEN*-distal *LYS4*, as described in Figure 3D. The percentage of cells lacking cohesion (sister separation) is shown. (C) Deletion of *WPL1* has little effect on the cohesion of *SMC3-MCD1* cells. *SMC3-MCD1* (VG3940-2D) and *SMC3-MCD1 wpl1*Δ (VG3957-1C) cells were synchronously arrested in mid-M-phase and scored for cohesion at the *CEN*-distal *LYS4* locus, as in Figure 3D. The percentage of cells lacking cohesion (sister separation) is shown.

cohesion defect as the *SMC3-MCD1* strain (Figure 4C). Together, these results suggest that Wpl1p promotes efficient cohesion through the destabilization of the Smc3p/Mcd1p interface.

Regulation of the Smc3p/Mcd1 interface, but not the Pds5p N-terminus, is important for resistance to DNA-damaging agents

The final characteristic *wpl1*Δ phenotype is their sensitivity to the DNA-damaging agents CPT and MMS. As our results suggested that the N-terminus of Pds5p and Wpl1p function together in cohesion and condensation, we wondered whether they also function together to promote DNA-damage repair. To test this possibility, we examined effects on the growth of the *pds5* N-terminal mutants alone or in the *wpl1*Δ background by plating the single- and double-mutants on media containing either CPT or MMS. Surprisingly, cells containing *pds5-S81R*, *pds5-P89L*, and *pds5-E181K* alone grew similarly to wild-type cells on 20 μg/ml CPT and 0.015% MMS, and significantly better than *wpl1*Δ cells. The *wpl1*Δ *pds5* double-mutants and *wpl1*Δ cells were equally sensitive to both CPT and MMS (Figure 5A). These results suggest that Wpl1p's role in DNA-damage repair is independent of its functional interaction with the Pds5p N-terminus.

We also tested whether the ability to modulate the Smc3p/Mcd1p interface was required for resistance to DNA-damaging agents. We compared the sensitivities of wild-type, *wpl1*Δ, and *SMC3-MCD1* fusion strains to 20 μg/ml CPT and to 0.01% MMS. The *SMC3-MCD1* fusion strain and the *wpl1*Δ strain showed similar growth inhibition to both drugs (Figure 5B). Together, our analyses of cells containing the Smc3-Mcd1p fusion protein suggest that Wpl1p destabilization of the Smc3p/Mcd1p interface is a common underlying mechanism necessary to promote the cohesion and repair of S-phase-induced DNA damage, as well as to inhibit condensation.

Physical interaction between Wpl1p and Pds5p is not sufficient for regulation of cohesin function

After determining that Wpl1p and the N-terminus of Pds5p share a common function in promoting cohesion and the inhibition of condensation, we sought to determine if these functions derive from formation of the Wpl1p-Pds5p complex. If so, *pds5* N-terminal mutants might abrogate formation of the Wpl1p-Pds5p complex. Support for this idea came from a recent crystal structure of human Pds5B (Ouyang *et al.* 2016). This crystal structure also contained a short peptide from the N-terminus of Wapl, the human ortholog of Wpl1p, which bound to the N-terminus of Pds5B. As this Pds5B region is highly conserved with yeast Pds5p, we were able to map the analogous residues of the Pds5p N-terminal mutations onto the crystal structure of Pds5B (Figure 6A and Figure S6 in File S1). These residues were located either within, or in very close proximity to, the Wapl-binding site (Figure 6A).

Given this structural information, we asked whether the Pds5p N-terminal mutations disrupted the physical interaction between Pds5p and Wpl1p. We C-terminally tagged Wpl1p with the Flag epitope (Wpl1p-3FLAG) and then performed anti-FLAG immunoprecipitation from extracts of asynchronously growing cells. We compared Wpl1p co-immunoprecipitation with wild-type Pds5p and each of the N-terminal Pds5p mutants. The anti-FLAG immunoprecipitation robustly co-immunoprecipitated wild-type Pds5p when Wpl1p-3FLAG was present, but not when Wpl1p was untagged, confirming

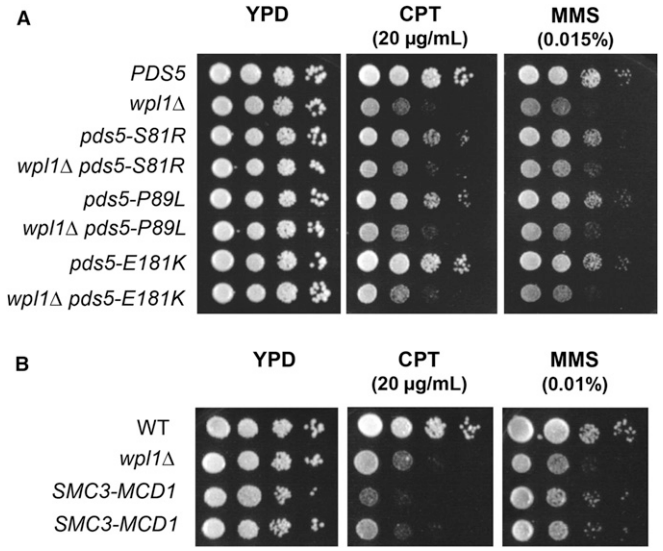

Figure 5 The *SMC3-MCD1* fusion, but not *pds5* N-terminal mutants, is defective for Wpl1p-mediated DNA repair. (A) Assessment of sensitivity of *pds5* N-terminal mutants to camptothecin (CPT) and MMS. Cultures of cells in the *WPL1* background [*PDS5* (VG3349-1B) *pds5-S81R* (MSB183-1A), *pds5-P89L* (MSB184-3A), and *pds5- E181K* (MSB101-3C)] and the *wpl1*Δ background [*wpl1*Δ (VG3360-3B), *pds5-S81R wpl1*Δ (MSB204-1B), *pds5-P89L wpl1*Δ (MSB205-4C), and *pds5-E181K wpl1*Δ (MSB223-1A)] were serially diluted 10-fold and plated on YPD media either containing no drug, 20 μg/ml CPT, or 0.015% MMS, and incubated at 23° and assessed at 3 days postplating. (B) Assessment of sensitivity of *SMC3-MCD1* fusion to CPT and MMS. Wild-type (*WT*) (VG3349-1B), *wpl1*Δ (VG3360-3B), and *SMC3-MCD1* (VG3940-2D) were serially diluted 10-fold and plated on YPD media alone, or containing either 20 μg/ml CPT or 0.01% MMS, then incubated at 23° and assessed 3 days postplating.

that Pds5p co-immunoprecipitation is due to a specific interaction with Wpl1p (Figure 6B). The Wpl1p-3FLAG immunoprecipitates contained very little Pds5p-P89L and clearly reduced amounts of Pds5p-E181K (Figure 6B). Thus, both mutations disrupt Pds5p binding to Wpl1p. In contrast, Pds5p-S81R retained binding to Wpl1p-3FLAG at a level similar to wild-type Pds5p (Figure 6B). These differences in Wpl1p binding between the three N-terminal Pds5p mutants are surprising, as all three mutants similarly disrupt promotion of cohesion and restore viability to *eco1* mutants through restoration of condensation. These results suggest that binding to the Pds5p N-terminus is required for Wpl1p's function as both an inhibitor of condensation and efficient promoter of cohesion. However, this interaction is not sufficient for these functions, as Pds5p-S81R binds Wpl1p-3FLAG at close to wild-type levels.

The three *pds5* mutants have similar functional defects *in vivo*, despite their differences in the ability to bind Wpl1p. These differences suggest that the molecular function of Wpl1p must be attenuated through a mechanism other than Pds5p binding. Thus, we wondered whether the interaction between Wpl1p and cohesin might be compromised in these mutants. We probed the Wpl1p-3FLAG immunoprecipitates for the cohesin subunit, Mcd1p. In the wild-type Pds5p strain, Mcd1p exhibited robust co-immunoprecipitation with Wpl1p (Figure 6B). In contrast, in all three Pds5p N-terminal mutant strains, there was reduced Mcd1p co-immunoprecipitation with Wpl1p (Figure 6B). We conclude from this result that formation of a functional Wpl1p-Pds5p complex is important for efficient recruitment of Wpl1p to cohesin. Additionally, Wpl1p was still able to interact with Mcd1p in the *pds5-P89L* mutant cells despite the Wpl1p interaction with Pds5p being abolished. This result indicates that Wpl1p can bind cohesin independently of Pds5p, which corroborates previous studies in yeast and other organisms that show that Wpl1p can interact directly with the cohesin subunit Scc3p/SA/STAG (Rowland *et al.* 2009; Shintomi and Hirano 2009).

In contrast to our conclusion that the Pds5p N-terminus functions with Wpl1p to inhibit condensation and promote cohesion, our studies suggest that Wpl1p promotes DNA repair independently of the Pds5p N-terminus. Consistent with this idea, *pds5-P89L* abrogates Wpl1p's interaction with Pds5p, but Wpl1p retains the ability to bind Mcd1p (Figure 6B). However, it is possible that DNA damage causes a modification to Pds5p or Wpl1p that promotes the formation of the Wpl1p-Pds5p complex. If so, the interaction between Wpl1p and Pds5p-P89L might be restored upon the induction of DNA damage. We assessed this possibility by treating asynchronously growing *PDS5 WPL1-3FLAG* and *pds5-P89L WPL1-3FLAG* cells with either DMSO or 20 μg/ml CPT for 3 hr. We immunoprecipitated Wpl1p in extracts from these cells and assayed for Pds5p binding. Wild-type Pds5p and Wpl1p co-immunoprecipitated at similar levels with or without CPT, whereas Pds5p-P89L remained unable to co-immunoprecipitate with Wpl1p under either condition (Figure 6C). These findings further corroborate our conclusion that Wpl1p promotes DNA-damage repair independently of its interaction with Pds5p.

Discussion

Previous studies in budding yeast have demonstrated roles for Wpl1p in promoting efficient sister chromatid cohesion and in inhibiting condensation (Guacci and Koshland 2012; Lopez-Serra *et al.* 2013). Here, we provide evidence for a biological function of Wpl1p in the timely repair of DNA damage in S-phase, beyond its roles in cohesion and condensation. We report that cells blocked for Wpl1p function grow slowly when they experience DNA damage induced during S-phase by CPT and MMS. This slow growth results from a delay in the onset of chromosome segregation, likely reflecting activation of the DNA damage checkpoint in G2/M because of slow repair of the damage. Consistent with this view, Wpl1p was shown to promote the timely repair of DSBs and homologous recombination in budding yeast meiotic chromosomes (Challa *et al.* 2016).

The defect in DNA repair in cells blocked for Wpl1p function cannot be explained by their partial cohesion defect. We showed that *pds5* N-terminal mutants have the same partial cohesion defect as *wpl1*Δ and *SMC3-MCD1* cells, yet these *pds5* mutants exhibit growth similar to wild-type cells when exposed to CPT and MMS. These results suggest that Wpl1p modulates a cohesin function in the repair of S-phase-induced DNA damage beyond simply its role in promoting sister chromatid cohesion. When DNA damage is induced in G2/M,

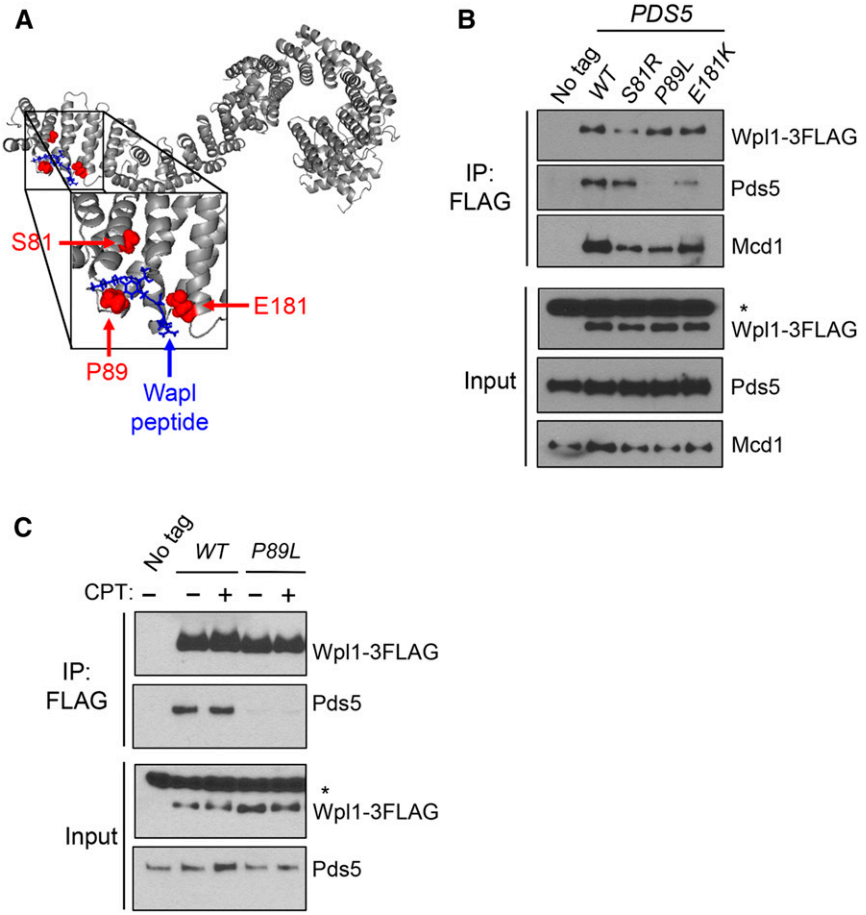

Figure 6 Pds5p N-terminus promotes Wpl1p binding to the cohesin complex. (A) Crystal structure of Pds5B bound to the YSR motif of Wapl from Ouyang *et al.* (2016). Gray: Pds5B; blue: Wapl peptide; red: *eco1-ts* suppressors from Rowland *et al.* (2009) and Sutani *et al.* (2009). Yeast residues were mapped to analogous residues on Pds5B through alignment. (B) Pds5p N-terminal mutants impair Wpl1p's binding to cohesin and but have different effects on Wpl1p's interaction with Pds5p. Wpl1p-3FLAG was immunoprecipitated from protein extracts in asynchronous cultures containing Wpl1p-3FLAG and either *PDS5* (MSB192-2A), *pds5-S81R* (MSB193-1B), *pds5-P89L* (MSB194-1C), or *pds5-E181K* (MSB195-2D), as described in the *Materials and Methods*. No tag control contains wild-type (*WT*) untagged *WPL1* and *PDS5* alleles (VG3349-1B). For western blot analysis, Wpl1p was detected using mouse anti-FLAG, Pds5p was detected using rabbit anti-Pds5, and Mcd1p was detected using rabbit anti-Mcd1 antibodies (*Materials and Methods*). For anti-FLAG, a nonspecific species present in all cells is denoted by an asterisk. (C) Assessment of interaction between Wpl1p-3FLAG and Pds5p (MSB192-2A) or Pds5p-P89L (MSB194-1C) when treated with CPT. Asynchronous cultures were treated either with DMSO or 20 μg/ml CPT for 3 hr before being harvested. No tag control is the *WPL1 PDS5* (VG3349-1B) strain, which was treated with DMSO. Immunoprecipitation (IP) and western blot analysis were performed as described in (B) and the *Materials and Methods*.

cohesin loading around the break site is stimulated (Ström *et al.* 2004; Unal *et al.* 2004). It may be that Wpl1p promotes cohesin binding at either sites of DNA damage or at replication forks to reinforce them upon damage, and thereby promotes DNA repair.

The results from our study suggest that Wpl1p regulates cohesin function in DNA repair, cohesion, and condensation through a common mechanism. We show that cells expressing the Smc3p-Mcd1p fusion protein, like *wpl1*Δ, have partial cohesion defects, are sensitive to S-phase DNA-damaging agents, and restore viability and condensation to cells lacking Eco1p. As Wpl1p destabilizes the interface between Smc3p and Mcd1p (Beckouët *et al.* 2016), the Smc3-Mcd1p fusion likely makes this interface refractory to Wpl1p function. The common phenotypes of *wpl1*Δ and the Smc3-Mcd1p fusion make it likely that Wpl1p-mediated regulation of the Smc3p/Mcd1p interface is required for efficient cohesion, timely repair of DNA damage, and the inhibition of condensation.

Disruption of the Smc3p/Mcd1p interface by Wpl1p is thought to be one mechanism to remove cohesin from DNA (Chan *et al.* 2012). Our results suggest that Wpl1p-mediated removal of cohesin has both positive (efficient promotion of cohesion and DNA repair) and negative (inhibition of condensation) consequences. One model posits that cohesin and Pds5p regulate chromosome condensation by first binding DNA at sites along a chromatid to divide the chromosomes into domains, followed by axial shortening generated by looping out the intervening DNA (Guacci *et al.* 1997; Hartman *et al.* 2000). Interactions between cohesins may contribute to condensation by mediating looping (Guacci *et al.* 1997; Hartman *et al.* 2000). Wpl1p may inhibit condensation by preventing or inhibiting cohesin from tethering DNA in *cis* along a chromatid. This process could entail either destabilizing interactions between nonacetylated cohesins and/or destabilize the DNA binding of nonacetylated cohesins (Figure 7A). Indeed, studies showed that Wpl1p depletion increased the size of DNA loops in interphase human cells, induced precocious condensation in human and yeast cells, and induced hyper-condensation in yeast mitotic and meiotic cells (Lopez-Serra *et al.* 2013; Tedeschi *et al.* 2013; Challa *et al.* 2016; Haarhuis *et al.* 2017). Moreover, the ability of *eco1*Δ *wpl1*Δ cells to condense their *rDNA* demonstrates that nonacetylated cohesin can promote condensation (Guacci and Koshland 2012). It is curious, though, that destabilization of cohesin's interaction with DNA would promote DNA repair and cohesion. These positive aspects may reflect cohesin's burden to carry out diverse biological functions.

Cohesin is loaded onto DNA at cohesion-associated regions prior to S-phase to establish cohesion, but cohesin is also loaded *de novo* at sites of damage and at stalled replication forks (Ström *et al.* 2004; Unal *et al.* 2004; Tittel-Elmer *et al.*

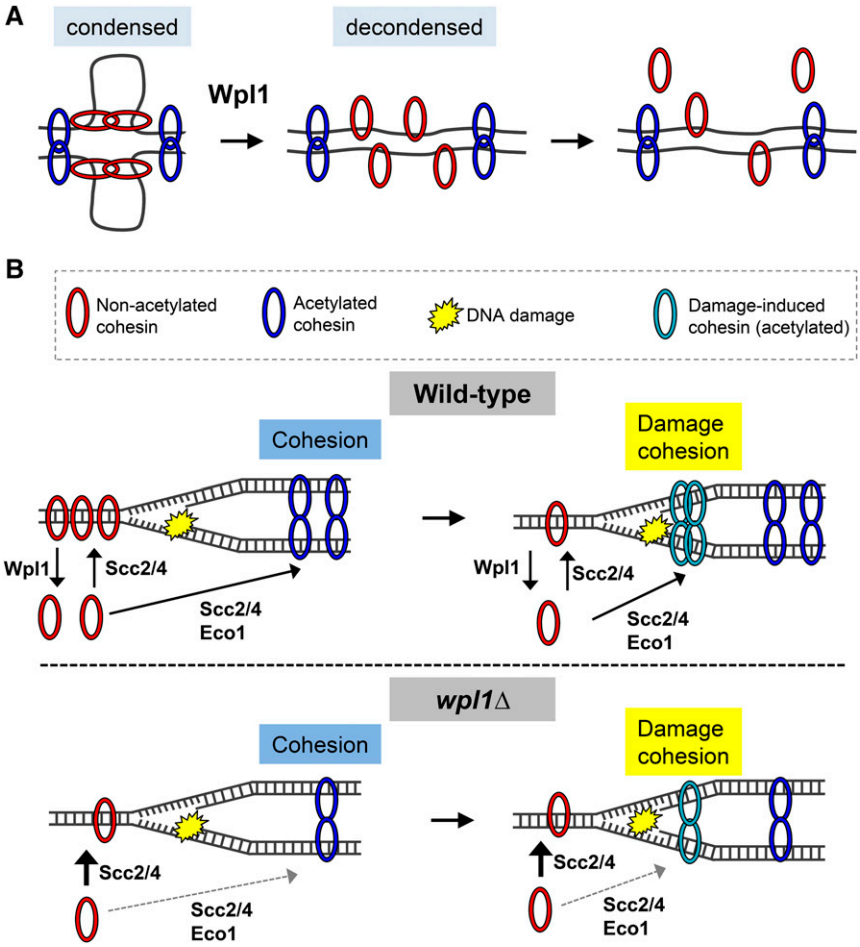

Figure 7 Model for Wpl1p promotion and inhibition of cohesin function through recycling. (A) Model for Wpl1p inhibition of condensation. Cohesin mediates condensation through chromosome looping. Nonacetylated cohesin (red) promotes condensation, while acetylated cohesin (blue) promotes cohesion. Wpl1p antagonizes condensation by countering interactions of nonacetylated cohesin and/or by removing nonacetylated cohesin from DNA. (B) Wpl1p promotes cohesion and DNA-damage repair. Top: when Wpl1p is present, nonacetylated cohesin (red) is loaded onto DNA by Scc2/4p, and is removed from DNA by Wpl1p, maintaining a soluble pool of cohesin. Cohesin loading, followed by Eco1p acetylation, promotes cohesion, which is refractory from Wpl1p. Upon DNA damage, nonacetylated cohesin is removed from other sites in the genome and/or is recruited from the soluble pool and loaded around the damage site. Bottom: in the absence of Wpl1p (*wpl1*Δ), cohesin is loaded onto DNA by Scc2/4p. The smaller amount of cohesin on DNA and in the soluble pool makes cohesion establishment less efficient or less robust. Upon DNA damage, cohesin removal from DNA and/or mobilization from the smaller soluble pool is limited. Thus, cohesin loading around damage sites is less efficient.

2012). These spatially and temporally distinct functions may require cohesin's mobilization, either from a DNA-bound or a nucleoplasm pool of cohesin (Figure 7B, top). In the absence of Wpl1p function, cohesin is stabilized on DNA, so is less efficiently mobilized and perhaps trapped in nonproductive sites. Additionally, *wpl1*Δ cells exhibit a twofold decrease in cohesin (Mcd1p) bound on DNA and in cells (Figure S7A in File S1; Rowland *et al.* 2009; Sutani *et al.* 2009; Guacci *et al.* 2015). In wild-type cells, most yeast cohesin is bound to chromosomes but a small soluble pool remains (Tóth *et al.* 1999; Tong and Skibbens 2014). *wpl1*Δ cells show decreases in both the chromosomal and soluble pools (Figure S7B in File S1). This decrease in cohesin levels in *wpl1*Δ cells may limit the pool of dynamic cohesin, regardless of whether it derives from a chromosomal or nucleoplasmic source. Thus, cohesion promotion is less efficient both during a normal cell cycle and in response to DNA damage (Figure 7B, bottom). We cannot rule out that the premature/hyper-condensation or aberrant chromosome structures in *wpl1*-depleted cells could contribute to DNA-damage sensitivity by hindering repair.

The necessity of maintaining a dynamic pool of cohesin is supported by a number of observations. First, only ~20–30% of cohesin is acetylated during S-phase to establish sister chromatid cohesion (Zhang *et al.* 2008). As acetylated cohesin is thought to be refractory to Wpl1p activity (Rolef Ben-Shahar *et al.* 2008; Unal *et al.* 2008), this small percentage of acetylated cohesin may ensure that most cohesin remains responsive to Wpl1p. Second, we previously showed that a three- to fourfold reduction in the total cellular pool of cohesin leads to more severe defects in condensation and DNA repair than in cohesion (Heidinger-Pauli *et al.* 2010). These phenotypes may arise from a larger proportion of the remaining cohesin being locked onto the DNA in the cohesive (acetylated) state that is refractory to Wpl1p, and thus not available for recycling to promote condensation and DNA repair. In this light, the primary biological function of Wpl1p may not be to inhibit cohesin's function by removing it from the DNA. Rather, it would be to generate a dynamic cohesin pool for redistribution to different chromosomal sites to perform cohesin's distinct biological functions.

The idea that Wpl1p mobilizes cohesin to perform different biological functions can explain two seeming paradoxes from our studies. First, we found that the three *pds5* N-terminal mutants dramatically differ in their ability to bind Wpl1p, yet mimic *wpl1*Δ in their failure to efficiently promote cohesion and inhibit condensation. Second, we found that all three *pds5* mutants differ from *wpl1*Δ in their resistance to DNA-damaging agents. As *wpl1*Δ cells and *pds5-P89L* cells exhibit the same almost twofold decrease in cohesin bound to chromosomes (Rowland

et al. 2009; Sutani *et al.* 2009; Guacci and Koshland 2012), the difference in sensitivity cannot be due to different levels of cohesin binding. However, these paradoxes may be explained by the similar reduction in the amount of Wpl1p bound to cohesin that we observed in the three *pds5* N-terminal mutants. The regulation of both cohesion and condensation entails the modulation of cohesin at many sites genome-wide. *pds5* N-terminal mutants may reduce the amount of Wpl1p bound to cohesin below a threshold required to mobilize the global pool of cohesin, thereby impairing the proper regulation of cohesion and condensation. In contrast, repair of DNA damage is likely to involve a small number of genomic sites, so may require a smaller pool of cohesin. The reduced levels of Wpl1p bound to cohesin in the *pds5* N-terminal mutants may be sufficient to mobilize enough cohesin to promote DNA repair. As there is no Wpl1p present in *wpl1*Δ cells, all three cohesin biological functions would be defective.

In addition to the insights into the relationship between Wpl1p and cohesin, our work furthers our understanding of the relationship between Wpl1p and Pds5p. Two *pds5* N-terminal alleles either entirely (*pds5-P89L*) or partially (*pds5-E181K*) disrupt the interaction with Wpl1p. However, Wpl1p still binds cohesin in these cells, albeit at reduced levels. These data suggest that one function of the Wpl1p-Pds5p complex is to help recruit Wpl1p to cohesin. However, Wpl1p can also bind cohesin independently of its ability to complex with Pds5p. This independence has previously been demonstrated *in vitro* (Rowland *et al.* 2009; Shintomi and Hirano 2009). The *pds5-S81R* mutation preserves the interaction between Pds5p and Wpl1p, yet its effects on cohesin function are the same as *pds5-P89L*, which abolishes this interaction. This result indicates that the formation of a Wpl1p-Pds5p complex is not sufficient for Wpl1p's function. The human Wapl N-terminus contains a conserved motif, [K/R][S/T]YSR, which has been shown to interact with the Pds5B N-terminus through crystal structure analysis (Figure 6A; Ouyang *et al.* 2016). This YSR motif is critical for the interaction between Wapl and Pds5B, and for Wapl function in vertebrate cells (Ouyang *et al.* 2016). The N-terminus of budding yeast Wpl1p contains a partial consensus of this motif, suggesting that Wpl1p may bind the yeast Pds5p N-terminus in a similar manner (Ouyang *et al.* 2016). As other cohesin regulators have also been shown to contain YSR-like motifs (Ouyang *et al.* 2016; Goto *et al.* 2017; Zhou *et al.* 2017), mutating the N-terminus of Pds5p may also compromise interaction with these factors, contributing to defects in cohesin function and regulation. We find that binding of Wpl1p to Pds5p requires interaction with the N-terminal Pds5p residues, but that this interaction is not sufficient for Wpl1p function. It may be that this complex must be activated, possibly through a conformational change in either one or both proteins for proper function, to enable interaction with other proteins.

Our studies provide new insights into how the Wpl1p-Pds5p complex regulates cohesin's functions *in vivo*. Our proposed role for Wpl1p in recycling cohesin, in part through its association with Pds5p, assigns a biological function for the previous finding that the Wpl1p-Pds5p complex promotes both cohesin loading and unloading *in vitro* (Murayama and Uhlmann 2015). Finally, exploring the roles of Wpl1p and cohesin in DNA-damage repair will open up an exciting new direction in the cohesin field.

Acknowledgments

We thank Rebecca Lamothe, Brett Robison, and Lorenzo Costantino for critical reading of the manuscript and helpful comments; Martin Kupiec, Anjali Zimmer, Jeremy Amon, Ryan Holly, Hugo Tapia, Kristian Carlborg, and Siheng Xiang for helpful discussion; Fiona Chatterjee for technical support; and Kim Nasmyth for kindly providing the *SMC3-MCD1* fusion construct to us. This work was supported by a National Institutes of Health grant (1R35 GM-118189-01 to D.K.)

Literature Cited

Avemann, K., R. Knippers, T. Koller, and J. M. Sogo, 1988 Camptothecin, a specific inhibitor of type-I DNA topoisomerase, induces DNA breakage at replication forks. Mol. Cell. Biol. 8: 3026–3034.

Beckouët, F., M. Srinivasan, M. B. Roig, K.-L. Chan, J. C. Scheinost *et al.*, 2016 Releasing activity disengages cohesin's Smc3/Scc1 interface in a process blocked by acetylation. Mol. Cell 61: 563–574.

Buheitel, J., and O. Stemmann, 2013 Prophase pathway-dependent removal of cohesin from human chromosomes requires opening of the Smc3-Scc1 gate. EMBO J. 32: 666–676.

Çamdere, G., V. Guacci, J. Stricklin, and D. Koshland, 2015 The ATPases of cohesin interface with regulators to modulate cohesin-mediated DNA tethering. Elife 4: 1–66.

Challa, K., M.-S. Lee, M. Shinohara, K. P. Kim, and A. Shinohara, 2016 Rad61/Wpl1 (Wapl), a cohesin regulator, controls chromosome compaction during meiosis. Nucleic Acids Res. 44: 3190–3203.

Chan, K.-L., M. B. Roig, B. Hu, F. Beckouët, J. Metson *et al.*, 2012 Cohesin's DNA exit gate is distinct from its entrance gate and is regulated by acetylation. Cell 150: 961–974.

Chan, K.-L., T. Gligoris, W. Upcher, Y. Kato, K. Shirahige *et al.*, 2013 Pds5 promotes and protects cohesin acetylation. Proc. Natl. Acad. Sci. USA 110: 13020–13025.

Ciosk, R., M. Shirayama, A. Shevchenko, T. Tanaka, A. Tóth *et al.*, 2000 Cohesin's binding to chromosomes depends on a separate complex consisting of Scc2 and Scc4 proteins. Mol. Cell 5: 243–254.

Eng, T., V. Guacci, and D. Koshland, 2014 ROCC, a conserved region in cohesin's Mcd1 subunit, is essential for the proper regulation of the maintenance of cohesion and establishment of condensation. Molecular Biology of the Cell 25: 2351–2364.

Feytout, A., S. Vaur, S. Genier, S. Vazquez, and J. P. Javerzat, 2011 Psm3 acetylation on conserved lysine residues is dispensable for viability in fission yeast but contributes to Eso1-mediated sister chromatid cohesion by antagonizing Wpl1. Mol. Cell. Biol. 31: 1771–1786.

Game, J. C., G. W. Birrell, J. A. Brown, T. Shibata, C. Baccari *et al.*, 2003 Use of a genome-wide approach to identify new genes that control resistance of Saccharomyces cerevisiae to ionizing radiation. Radiat. Res. 160: 14–24.

Gandhi, R., P. J. Gillespie, and T. Hirano, 2006 Human Wapl is a cohesin-binding protein that promotes sister-chromatid resolution in mitotic prophase. Curr. Biol. 16: 2406–2417.

Gligoris, T. G., J. C. Scheinost, F. Bürmann, N. Petela, K.-L. Chan *et al.*, 2014 Closing the cohesin ring: structure and function of its Smc3-kleisin interface. Science 346: 963–967.

Goto, Y., Y. Yamagishi, M. Shintomi-Kawamura, M. Abe, Y. Tanno *et al.*, 2017 Pds5 regulates sister-chromatid cohesion and chromosome bi-orientation through a conserved protein interaction module. Curr. Biol. 27: 1005–1012.

Gruber, S., P. Arumugam, Y. Katou, W. Helmhart, K. Shirahige *et al.*, 2006 Evidence that loading of cohesin onto chromosomes involves opening of its SMC hinge. Cell 127: 523–537.

Guacci, V., and D. Koshland, 1994 Chromosome condensation and sister chromatid pairing in budding yeast. J. Cell Biol. 125: 517–530.

Guacci, V., and D. Koshland, 2012 Cohesin-independent segregation of sister chromatids in budding yeast. Mol. Biol. Cell 23: 729–739.

Guacci, V., A. Yamamoto, A. Strunnikov, J. Kingsbury, E. Hogan *et al.*, 1993 Structure and function of chromosomes in mitosis of budding yeast. Cold Spring Harb. Symp. Quant. Biol. 58: 677–685.

Guacci, V., D. Koshland, and A. Strunnikov, 1997 A direct link between sister chromatid cohesion and chromosome condensation revealed through the analysis of MCD1 in S. cerevisiae. Cell 91: 47–57.

Guacci, V., J. Stricklin, M. S. Bloom, X. Guō, M. Bhatter *et al.*, 2015 A novel mechanism for the establishment of sister chromatid cohesion by the ECO1 acetyltransferase. Mol. Biol. Cell 26: 117–133.

Haarhuis, J. H. I., R. H. van der Weide, V. A. Blomen, J. O. Yáñez-Cuna, M. Amendola *et al.*, 2017 The cohesin release factor WAPL restricts chromatin loop extension. Cell 169: 693–707.e14.

Hartman, T., K. Stead, D. Koshland, and V. Guacci, 2000 Pds5p is an essential chromosomal protein required for both sister chromatid cohesion and condensation in Saccharomyces cerevisiae. J. Cell Biol. 151: 613–626.

Hartwell, L. H., 1974 Saccharomyces cerevisiae cell cycle. Bacteriol. Rev. 38: 164–198.

Heidinger-Pauli, J. M., O. Mert, C. Davenport, V. Guacci, and D. Koshland, 2010 Systematic reduction of cohesin differentially affects chromosome segregation, condensation, and DNA repair. Curr. Biol. 20: 957–963.

Kueng, S., B. Hegemann, B. H. Peters, J. J. Lipp, A. Schleiffer *et al.*, 2006 Wapl controls the dynamic association of cohesin with chromatin. Cell 127: 955–967.

Lopez-Serra, L., A. Lengronne, V. Borges, G. Kelly, and F. Uhlmann, 2013 Budding yeast Wapl controls sister chromatid cohesion maintenance and chromosome condensation. Curr. Biol. 23: 64–69.

Michaelis, C., R. Ciosk, and K. Nasmyth, 1997 Cohesins: chromosomal proteins that prevent premature separation of sister chromatids. Cell 91: 35–45.

Murayama, Y., and F. Uhlmann, 2015 DNA entry into and exit out of the cohesin ring by an interlocking gate mechanism. Cell 163: 1628–1640.

Noble, D., M. Kenna, M. Dix, R. V. Skibbens, and E. Unal, 2006 Intersection between the regulators of sister chromatid cohesion establishment and maintenance in budding yeast indicates a multi-step mechanism. Cell Cycle 5: 2528–2536.

Onn, I., J. M. Heidinger-Pauli, V. Guacci, E. Unal, and D. Koshland, 2008 Sister chromatid cohesion: a simple concept with a complex reality. Annu. Rev. Cell Dev. Biol. 24: 105–129.

Ouyang, Z., G. Zheng, D. R. Tomchick, X. Luo, and H. Yu, 2016 Structural basis and IP6 requirement for Pds5-dependent cohesin dynamics. Mol. Cell 62: 248–259.

Panizza, S., T. Tanaka, A. Hochwagen, F. Eisenhaber, and K. Nasmyth, 2000 Pds5 cooperates with cohesin in maintaining sister chromatid cohesion. Curr. Biol. 10: 1557–1564.

Rolef Ben-Shahar, T., S. Heeger, C. Lehane, P. East, H. Flynn *et al.*, 2008 Eco1-dependent cohesin acetylation during establishment of sister chromatid cohesion. Science 321: 563–566.

Rowland, B. D., M. B. Roig, T. Nishino, A. Kurze, P. Uluocak *et al.*, 2009 Building sister chromatid cohesion: Smc3 acetylation counteracts an antiestablishment activity. Mol. Cell 33: 763–774.

Saleh-Gohari, N., H. E. Bryant, N. Schultz, K. M. Parker, T. N. Cassel *et al.*, 2005 Spontaneous homologous recombination is induced by collapsed replication forks that are caused by endogenous DNA single-strand breaks. Mol. Cell. Biol. 25: 7158–7169.

Shintomi, K., and T. Hirano, 2009 Releasing cohesin from chromosome arms in early mitosis: opposing actions of Wapl-Pds5 and Sgo1. Genes Dev. 23: 2224–2236.

Skibbens, R. V., L. B. Corson, D. Koshland, and P. Hieter, 1999 Ctf7p is essential for sister chromatid cohesion and links mitotic chromosome structure to the DNA replication machinery. Genes Dev. 13: 307–319.

Stead, K., C. Aguilar, T. Hartman, M. Drexel, P. Meluh *et al.*, 2003 Pds5p regulates the maintenance of sister chromatid cohesion and is sumoylated to promote the dissolution of cohesion. J. Cell Biol. 163: 729–741.

Ström, L., H. B. Lindroos, K. Shirahige, and C. Sjögren, 2004 Postreplicative recruitment of cohesin to double-strand breaks is required for DNA repair. Mol. Cell 16: 1003–1015.

Ström, L., C. Karlsson, H. B. Lindroos, S. Wedahl, Y. Katou *et al.*, 2007 Postreplicative formation of cohesion is required for repair and induced by a single DNA break. Science 317: 242–245.

Strumberg, D., A. A. Pilon, M. Smith, R. Hickey, L. Malkas *et al.*, 2000 Conversion of topoisomerase I cleavage complexes on the leading strand of ribosomal DNA into 5′-phosphorylated DNA double-strand breaks by replication runoff. Mol. Cell. Biol. 20: 3977–3987.

Sutani, T., T. Kawaguchi, R. Kanno, T. Itoh, and K. Shirahige, 2009 Budding yeast Wpl1(Rad61)-Pds5 complex counteracts sister chromatid cohesion-establishing reaction. Curr. Biol. 19: 492–497.

Tanaka, K., Z. Hao, M. Kai, and H. Okayama, 2001 Establishment and maintenance of sister chromatid cohesion in fission yeast by a unique mechanism. EMBO J. 20: 5779–5790.

Tedeschi, A., G. Wutz, S. Huet, M. Jaritz, A. Wuensche *et al.*, 2013 Wapl is an essential regulator of chromatin structure and chromosome segregation. Nature 501: 564–568.

Tittel-Elmer, M., A. Lengronne, M. B. Davidson, J. Bacal, P. François *et al.*, 2012 Cohesin association to replication sites depends on Rad50 and promotes fork restart. Mol. Cell 48: 98–108.

Tong, K., and R. V. Skibbens, 2014 Cohesin without cohesion: a novel role for Pds5 in Saccharomyces cerevisiae. PLoS One 9: e100470.

Tóth, A., R. Ciosk, F. Uhlmann, M. Galova, A. Schleiffer *et al.*, 1999 Yeast cohesin complex requires a conserved protein, Eco1p(Ctf7), to establish cohesion between sister chromatids during DNA replication. Genes Dev. 13: 320–333.

Unal, E., A. Arbel-Eden, U. Sattler, R. Shroff, M. Lichten *et al.*, 2004 DNA damage response pathway uses histone modification to assemble a double-strand break-specific cohesin domain. Mol. Cell 16: 991–1002.

Unal, E., J. M. Heidinger-Pauli, and D. Koshland, 2007 DNA double-strand breaks trigger genome-wide sister-chromatid cohesion through Eco1 (Ctf7). Science 317: 245–248.

Unal, E., J. M. Heidinger-Pauli, W. Kim, V. Guacci, I. Onn *et al.*, 2008 A molecular determinant for the establishment of sister chromatid cohesion. Science 321: 566–569.

Zhang, J., X. Shi, Y. Li, B.-J. Kim, J. Jia *et al.*, 2008 Acetylation of Smc3 by Eco1 is required for S phase sister chromatid cohesion in both human and yeast. Mol. Cell 31: 143–151.

Zhou, L., C. Liang, Q. Chen, Z. Zhang, B. Zhang *et al.*, 2017 The N-terminal non-kinase-domain-mediated binding of Haspin to Pds5B protects centromeric cohesion in mitosis. Curr. Biol. 27: 992–1004.

Communicating editor: N. Hunter